Shape-Specific Iron Platinum Nanocrystals for Spin-Transfer Torque in Magnetic Tunnel Junctions

Kai He
Electrical and Computer Engineering, Rice University

NNIN REU Site: Microelectronics Research Center, The University of Texas, Austin, TX
NNIN REU Principal Investigator: Prof. Sanjay Banerjee, Electrical and Computer Engineering, University of Texas at Austin
NNIN REU Mentor: Dr. Domingo Ferrer, Electrical and Computer Engineering, University of Texas at Austin
Contact: kai.he@rice.edu, banerjee@ece.utexas.edu, domingo@mer.utexas.edu

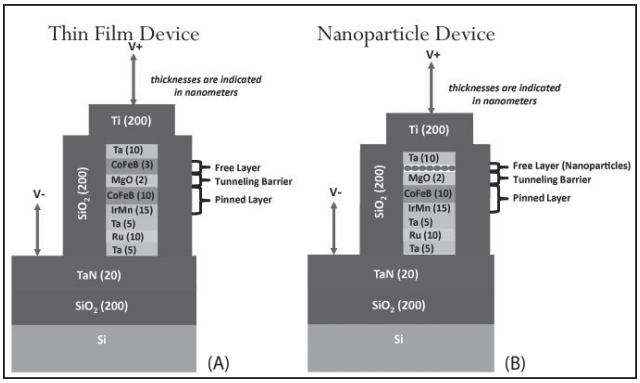

Figure 1: (A) Thin film device stack. (B) Nanoparticle device stack.

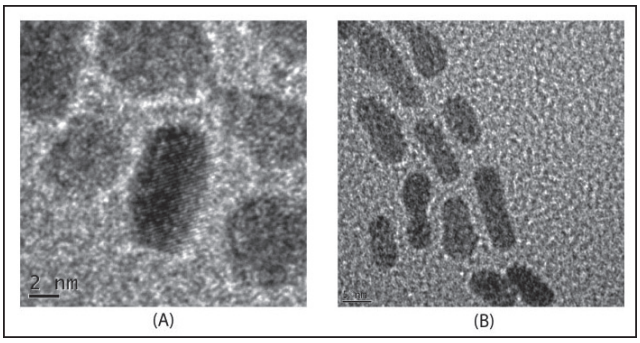

Figure 2: Transmission electron microscope images of (A) obloids and (B) nanowires.

Abstract and Introduction:

Using magnetic states for data storage has the advantages of nonvolatile storage bits, nondestructive read/write operations, and no wear-out mechanism [1]. We fabricated spin transfer torque magnetic tunnel junctions (STT-MTJ's); bit level devices of spin transfer torque random access memory (STTRAM). These devices have a ferromagnet / dielectric / ferromagnet top to bottom construction and operate on the principle of tunneling magnetoresistance. Resistance of the junction varied depending on the relative orientation of the spins in the magnetization directions of the ferromagnetic layers. Parallel alignment displayed low resistance, while antiparallel ordering portrayed high resistance [2].

High anisotropy, chemical and thermal stability, and tunable morphology of iron platinum (FePt) nanocrystals make them attractive for STTRAM applications. This project sought to assess the viability of replacing the top ferromagnet layer with ferromagnetic FePt nanocrystals (Figure 1b).

Bias dependence of differential resistance and tunneling magnetoresistance were also investigated on magnetic tunneling junctions (MTJs) with an ultrathin magnesium oxide (MgO) tunnel barrier (~20Å) fabricated via atomic layer deposition (ALD) (Figure 1a).

Nanocrystal Synthesis and Device Fabrication:

Nanocrystals were synthesized by reduction of platinum acetylacetonate and thermal decomposition of iron pentacarbonyl. Oleylamine and oleic acid were used as surfactants. Shape was controlled by varying solvents, sequence of surfactant addition, and reaction temperatures. We synthesized obloids and nanowires for the MTJ's.

To create obloids (Figure 2a) 0.192g platinum acetylacetonate, 10 ml benzyl ether, and 5 ml octadecene were added to a three-necked flask and stirred at 45°C for one hour. Next, the reaction was heated to 120°C followed by the immediate addition of 0.15 ml iron pentacarbonyl and 1.6 ml oleic acid. Five minutes later, 1.65 ml oleylamine was added. The reaction was then heated to 200°C and held for two hours [3].

To yield nanowires (Figure 2b) 0.098g platinum acetylacetonate, 100 mg 1,2-hexadecanediol, and 10 ml of oleylamine were added to a three-necked flask and stirred at room temperature for 20 minutes. The reaction was heated to 100°C and 10 μL iron pentacarbonyl was added. After holding the temperature at 100°C for the next 20 minutes, 2 ml oleic acid was injected. The reaction was heated to 300°C and held there for 30 minutes [3]. Both reactions ran under a nitrogen atmosphere.

The devices were fabricated on a silicon wafer by depositing silicon dioxide (SiO_2) through evaporation, tantalum nitrite (TaN) using sputtering, and SiO_2. Wells of 70 × 70 nm^2, 100 × 100 nm^2, and 200 × 200 nm^2 for the stacks were patterned in the top SiO_2 layer using electron-beam

(e-beam) lithography and dry etched afterwards. The stack was sputtered, with the exception of the MgO layer where ALD was used.

In the future, the nanoparticle device-free layer (nanoparticles) will be attached by first immersing the wafer in a 20 mg/ml poly(ethyleneimine) (PEI) solution in chloroform for five minutes followed by immersion in a 1 mg/ml nanoparticle solution for 20 minutes [4].

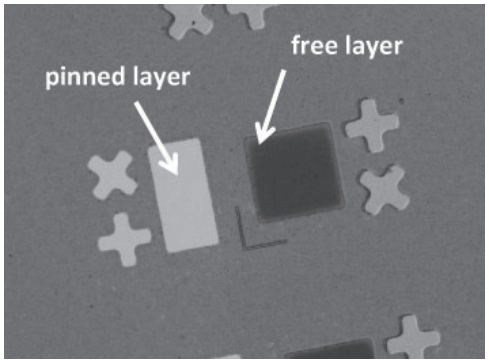

Figure 3: Finished thin film device.

Top and bottom electrodes were patterned using photolithography. The top electrode was created through evaporation of titanium followed by lift-off. RIE was used to define the underlying TaN bottom electrode.

We have only finished fabricating the proposed thin film devices (Figure 3) by the time of submission of this report. The nanoparticle device wafer has been patterned by e-beam and awaits stack deposition.

Results and Future Work:

FePt nanoparticle magnetic properties were measured by sweeping an applied magnetic field and then acquiring magnetic moment data via a superconducting quantum interference device (SQUID) magnetometer. Both unannealed and annealed obloidal samples showed a discernable hysteresis. Annealing put the FePt into a more ordered L10 state and as Figure 4c shows, the annealed sample had higher magnetic moment when exposed to applied fields of comparable magnitude as the unannealed samples. Nanoparticles with an L10 structure were required for room temperature device operation.

We have preliminary thin film device data made through a two point probe. Resistance measurements were made after biasing the device in the range of -1V to 1V (Figure 4b), as well as after applying varying pulse amplitudes (Figure 4d). Biasing the device showed a higher resistance on the voltage up-sweep than the down-sweep. Pulsing currents of increasing amplitudes decreased the resistance of the junction. Then pulsing currents of decreasing amplitude switched the device back into a higher resistance state.

This data shows a clear hysteresis in the switching characteristic of the device. Both tests suggest switching. However, in further pulse testing, the device resistance proved difficult to switch back from low resistance (parallel state) into the high resistance state (antiparallel state). This was perhaps due to the oxidation of the top titanium electrode.

In the future, we would like to confirm this is indeed the case by changing the top electrode to copper or gold. Additional work includes implementation of nanoparticle devices and verification of their functionality. Comparisons of switching critical current and switching speed in these thin-film and nanoparticle devices also stand as future goals.

Acknowledgements:

I thank Prof. Sanjay Banerjee and Dr. Domingo Ferrer for their guidance and opportunity to work with them this summer. I also want to thank the Banerjee group, in particular Samaresh Guchhait, Urmimala Roy, Soheil Gharahi, Archana Rai, and Prateek Gadkari for their efforts. I also thank the NNIN REU Program and the NSF for organizing and funding this experience.

References:

[1] Ferrer, D. A.; "Origin of shape anisotropy effects in solution-phase synthesized FePt nanomagnets"; J. Appl. Phys. 110, 014316 (2011).

[2] Slaughter, J.; "Materials for Magnetoresistive Random Access Memory"; Annual Review of Materials Research, Vol. 39, 277-296 (2009).

[3] Narayan P.; "Shape control of FePt nanocrystal"; J. Appl. Phys. 105, 07A749 (2009).

[4] Yildirim, O.; "Monolayer-directed Assembly and Magnetic Properties of FePt Nanoparticles on Patterned Aluminum Oxide"; International Journal of Molecular Sciences, 11. pp. 1162-1179 (2010).

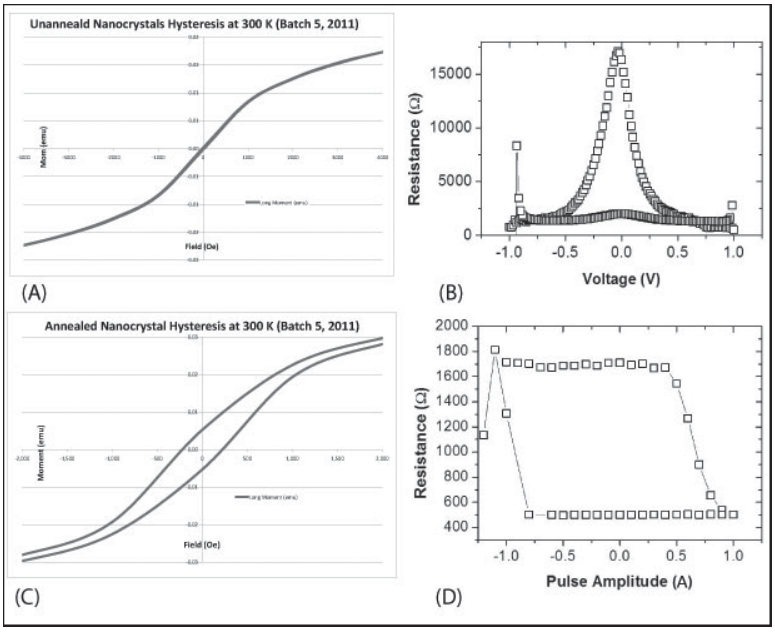

Figure 4: SQUID data for (A) unannealed and (C) annealed obloid nanoparticles show ferromagnetism. Resistance measurements made after (B) voltage sweeps and (D) current pulses of increasing amplitude show device switching.